TWELFTH EUROPEAN ROTORCRAFT FORUM

Paper No. 20

FREE WAKE ANALYSIS OF COMPRESSIBLE ROTOR FLOW FIELDS IN HOVER

John Steinhoff and
K. Ramachandran

The University of Tennessee Space Institute
Tullahoma, Tennessee, U.S.A.

September 22–25, 1986

Garmisch-Partenkirchen
Federal Republic of Germany

Deutsche Gesellschaft für Luft- und Raumfahrt e. V. (DGLR)
Godesberger Allee 70, D-5300 Bonn 2, F.R.G.

Free Wake Analysis of Compressible Rotor Flow Fields in Hover*

John Steinhoff†*
K. Ramachandran‡*

The University of Tennessee Space Institute
Tullahoma, Tennessee

Abstract

In the computation of helicopter rotor flow fields, it is well known that wake effects can be very important. In addition, compressibility can be very important since, at the speeds of modern rotors, shocks can start to appear near the blade tip.

Extensive work has been done on incompressible rotor flows using vortex tracking methods to follow the wake for free wake analyses. These, of course, cannot treat compressibility effects. On the other hand, extensive work has also been done for fixed wings in transonic flow, using compressible potential flow and Euler equation methods. This work may have problems if used for free wake analysis of rotor flows due to the inability of potential flow solvers as currently used to allow a free wake, and Euler solvers to propagate the wake over significant distances without numerical diffusion and spreading.

In this paper we describe a unified method that is fully compressible, and which computes the wake without requiring external specification of the wake, or separate computations for the wake and blade region. This method has been developed into a computer program ("**HELIX I**") for the computation of compressible rotor flow fields in hover with free wakes. Results of this program are also described. The method utilizes a modification of a compressible finite volume potential flow technique. This technique has been extensively used in the fixed-wing industry for research and wing design, and has been shown to be effective for resolving shocks and to be in good agreement with experiment for subsonic and transonic flows. We obtain similar agreement for rotor flow field solutions, as shown by computed surface pressure plots. In addition, with our new wake treatment, we are able to compute wake positions that are in substantial agreement with experiment.

* Supported by ARO Contract DAAG29-K0019
* †Associate Professor
* ‡Graduate Research Associate

1. Introduction

In the computation of helicopter rotor flow fields, wake effects can be very important, since each blade passes close to the wake produced by the preceding ones, causing a large local effect. Also, the vortical flow from the wake of a number of blade passages can accumulate and cause a large global effect. In addition to wake effects, compressibility can be very important since, at the speeds of modern rotors, shocks can start to appear near the blade tip.

Extensive work has been done on incompressible rotor flows using vortex tracking methods to follow the wake for free wake analyses. These, of course, cannot treat compressibility effects. On the other hand, extensive work has also been done for fixed wings in transonic flow, using compressible potential flow and Euler equations. This work may have problems when used for free wake analysis of rotor flows due to the inability of potential flow solvers as currently used to allow a free wake, and Euler solvers to propagate the wake over significant distances without numerical diffusion and spreading. As a result of these problems, rotor calculations using these methods have been mainly restricted to the region near the blade.[1] A separate, usually Biot Savart, calculation of the wake has then been done. The two calculations are then coupled through specification of the boundary conditions on the near-blade grid.

We feel that it would be desirable to have a unified method that computes compressible rotor flows with free wakes using a single grid system and set of flow equations for the blade and wake region.

2. Basic Method

Compressible potential flow methods have been successfully used for both low and high speed external flow calculations, including transonic cases with shocks and flows over complex geometries. They typically involve a fixed computational grid on which a single set of equations, expressing mass balance, is solved for a single variable (potential). The velocity computed from this potential not only satisfies mass balance, but also the other Euler equations expressing momentum conservation in regions of the flow where there is no vorticity. Conventional potential flow methods include vorticity effects by specifying a surface across which the potential is discontinuous. This surface is a coordinate surface of the computational grid. Although momentum is conserved in the rest of the field (except when there are very strong shocks), it is not in general conserved across this surface of discontinuity. Accordingly, the solution is not accurate in this region. Also, if multiple vortex sheets are present, unless they are properly treated, there can be large errors extending throughout the entire flow field. For rotors much of the flow region has no vorticity, but thin regions of concentrated vorticity exist in the wakes of the blades and have a large effect on the flow. Thus, conventional potential flow methods are not suitable for a unified treatment of helicopter rotor flow.

Our basic approach involves modifying the potential flow wake treatment so that, within the numerical approximation, momentum is conserved there, as in the rest of the field. The internal structure of the vortex is not solved for, but is modeled and spread over several grid points. The wake position and vorticity strength are computed so that

momentum over the wake is balanced in an integral sense. Using momentum equations in the form of Crocco's relation, streamlines outside the wake which have no vorticity upstream, must not cross the wake, where there is vorticity. Thus, the wake remains sandwiched between sets of irrotational streamlines, extending downstream from either side of the rotor blade trailing edge. This defines the wake position. The vorticity within the wake is defined by the requirements of vorticity conservation and pressure balance, which also result from the momentum equations. This formulation allows the internal structure of the wake, which is largely determined by viscous effects, to be specified, if it is important to do so. This internal structure, which has a much smaller scale than other features of the flow, is not solved for by the finite difference method, and large numbers of grid points need not be dedicated to resolving it. Also, as in flows with shocks or axially symmetric straight vortex lines, it may be true that the internal structure has little influence on the flow outside the internal regions, as long as overall conservation laws are enforced. Then, even very crude, *ad hoc* internal profiles may be used. This possibility has to be checked, although preliminary calculations indicate that it is true.

We first decompose the velocity into a free stream, potential and vortical part:

$$\vec{q} = \vec{q}_\infty + \vec{\nabla}\phi + \vec{q}^{\,v} \tag{1}$$

The vortical part: $\vec{q}^{\,v}$, is concentrated near the sheet. A fixed grid (in the rotating blade-fixed frame) is used to solve the compressible potential flow equation for the potential, ϕ:

$$\partial_x(\rho u) + \partial_y(\rho v) + \partial_z(\rho w) = 0 \tag{2}$$

where ρ is the density and has the isentropic form away from the sheet. The density is based on the total velocity, $\vec{q}$, as are the components u, v and w. The vortical component, $\vec{q}^{\,v}$, is spread over several grid points around the vortex sheet so that vorticity is concentrated there.

During iteration towards convergence (the solution is steady in the blade coordinate system for hover) a four step procedure is repeatedly used:

1) The vortex sheet position is integrated as a set of marker streamlines to follow the flow using interpolated values of $\vec{q}$ from the fixed grid;

2) $\vec{q}^{\,v}$ is computed at grid points near the sheet;

3) a potential, ϕ, is computed at each grid point to satisfy eqn. (2);

4) a new velocity ($\vec{q}$) is computed at each grid point based on eqn. (1).

At convergence eqn. (2) is satisfied and the vortex sheet follows the flow. This process is described in detail in Refs. (2) and (3).

Although the vortex sheet is effectively spread over several grid points there is no cumulative numerical diffusion and the spreading remains fixed at its input value. Thus, the internal structure of the sheet is modeled rather than computed. As opposed to prescribed wake methods, in our method the wake system is not modeled but solved for, while only the internal structure is modeled. Thus, experimental or theoretical information can, if desired, be inserted into the method to prescribe this internal structure, while no

experimental information is needed for the wake position. This is similar to boundary layer methods which are used for flow over wing surfaces and coupled to potential flow methods. It will be seen that good results can be obtained with a very crude internal structure model requiring no inputs from experiment or parameter adjustments to fit data. Our method can be contrasted to the use of Euler or Navier Stokes equations on fixed grids: For meshes that are currently feasible, the wake spreads with these methods.

3. Results

Results are presented for the full solution of a lifting rotor in hover, as computed by the three dimensional compressible flow code, **HELIX I**. Previous results of the method, published elsewhere, described a line vortex propagating past a three dimensional wing[2], and subsequently, a point vortex convecting past a two dimensional airfoil[3], and a vortex sheet rolling up in a parabolized approximation[4]. In Fig. 1 preliminary results of the full three dimensional compressible code are presented for a single vortex sheet shed by a rotor blade. Here, the velocity in a cross-plane normal to the motion behind the trailing edge is presented. The cross-stream velocity clearly shows a tight vortex which is the size specified by the model used (gaussian distribution). This remains the same size as it is convected downstream. Other internal vortex structures and density distributions consistent with the grid spacing could also be imposed. For this case an untwisted Joukowski profile was used with a pitch of 5^o and an aspect ratio of 19. Figure 2 depicts the inner position of the grid used in our program, with periodic coordinates in Θ in the far field, for cases to be described below involving an NACA0012 profile at an 8^o pitch. A similar grid was used for the Joukowski profile.

In Fig. 3 the computed downward motion and contraction of the centroid of the tip vortex along the sheet for the full vortex system is presented (as a solid line) as a function of rotor angle, for the 5^o Joukowski blade. Figs. 4 – 8 depict the computed sheet position (defined by markers) 35 degrees after passage of the blade (positions of sheets 5 – 7 are extrapolated to reduce computing time). Also, Figs. 4 and 5 depict vorticity contours for the separate contribution of each individual sheet for relative values of .70 – .45 (in the same plane). The contour values are chosen to show the effects of the individual sheets as well as the spreading. Figures 6 – 8 present vorticity contours for the total vorticity field, which is a sum of the individual sheet contributions. Fig. 9 presents the computed circulation on the blade.

Figures 10 – 14 present computed results for a rotor with an aspect ratio of 18.2, constant NACA0012 cross section, no twist, pitch of 8^o and a tip Mach number of .61. These conditions match the experimental ones published in Ref. (5). In Fig. 10 the computed bound circulation is presented. In Figs. 11 and 12 the computed vertical motion and contraction of the tip vortex (calculated as the centroid of the computed vortex sheet) are presented, and compared with experimental results of Ref. (5). The comparison is seen to be fairly close, even though no adjustable parameters were used in the calculation. In Figs. 13 and 14 computed C_p distributions are presented at 68% and 89% span, respectively.

In Figs. 15 – 17 the circulation and vortex geometry are presented for the same blade and pitch, but aspect ratio of 6.0 and tip Mach number of .436. The experimental vortex

geometry of Ref. 6 for the same case is also presented in Figs. 16 and 17. The agreement is seen to be good. In Figs. 18 and 19 the C_p distribution is presented at 68% and 89% span together with experimental data of Ref.6. Again, agreement is good. In Fig. 20 the vortex sheet cross section geometry is presented 35 degrees after passage of the blade together with constant-vorticity contours. Our computed thrust coefficient of .0046 compares well with the experimental value of .0047.

A final case involves a NACA0012 2–bladed rotor with an 8^o pitch, aspect ratio of 6.0 and transonic tip Mach number of .877. The computed bound circulation is presented in Fig. 21, vortex vertical motion in Fig. 22 and contraction in Fig. 23. In Figs. 24 – 27 computed C_p values are presented and compared with experimental data for r/R values of .68, .80, .89 and .96, respectively. The comparison can be seen to be good except in the .96 case, which is very close to the tip. To resolve this region a finer grid is required there. Also, the relatively coarse grid used near the tip results in a vortex width there which is larger than experiment (although this width does not increase as the vortex convects). This can be seen in Figs. 11, 17 and 23 where the vortex centroid does not start at the tip of the rotor, but slightly inboard. Also, the starting vortex width can be inferred from the circulation distributions of Figs. 10, 15, and 21.

The (Neumann) conditions on the lower computational boundary (y = - .80) are chosen to represent an image system of vortices (with the same sign) between y = - .80 and y = −1.60, together with a semi-infinite vortical cylinder extending downward from y = −1.60. The (Dirichlet) conditions on the upper computational boundary represent a semi-infinite vortical cylinder extending downward from y = 0. The closed-form approximate solution presented in Ref.7 for the potential was used at these boundaries. These boundaries may be close enough to the blade to have some influence on the computed results. Sensitivity studies are being done on the influence of boundary position as well as vortex spreading.

4. Conclusion

A method has been described to compute the three dimensional flow over a helicopter rotor in hover, including compressibility and wake effects. The method requires no external data or parameter adjustments to define the wake position or other features of the flow. Only the blade geometry and rotational speed are required as inputs. The method has been implemented in a code, **HELIX I**. Results presented indicate good agreement with experiment for wake descent and contraction, as well as surface pressure distributions and thrust coefficients. These results include both high and low aspect ratio blades, and subsonic and transonic flows, including shocks.

Acknowledgement

Dr. Frank Caradonna of the Army Aeroflightdynamics Directorate at NASA–Ames provided extensive insight and help during this investigation. Also, the computing facilities there were used extensively. Mr. S. Nayani of UTSI contributed to the initial development of the code.

References

1. F. X. Caradonna and R. C. Strawn, "Numerical Modeling of Rotor Flows with a Conservative Form of the Full – Potential Equations," AIAA Paper 86–0079, AIAA 24^{th} Fluid and Plasma Dynamics Conference, January, 1986, Reno, Nevada.
   Also: R. Agarwal and J. Deese, "Euler Calculations for Flowfield of a Helicopter Rotor in Hover," presented at AIAA 4^{th} Applied Aerodynamics Conference, San Diego, California, June, 1986.

2. J. Steinhoff, K. Ramachandran and K. Suryanarayana, "The Treatment of Convected Vortices in Compressible Potential Flow." AGARD Symposium on Aerodynamics of Vortical Type Flows in Three Dimensions," pg. 22–1, (AGARD–CPP–342) Rotterdam, Netherlands, April, 1983.

3. W. J. McCroskey, and P. Goorjian, "Interactions of Airfoils with Gusts and Concentrated Vortices in Unsteady Transonic Flow," AIAA Paper 83–1691, AIAA 16^{th} Fluid and Plasma Dynamics Conference, July 1983, Danvers, Mass.

4. J. Steinhoff and K. Suryanarayana, "The Treatment of Vortex Sheets in Compressible Potential Flow," Page 1, Proceedings, AIAA Symposium on Computational Fluid Dynamics, Danvers, MA July 1983.

5. A. J. Landgrebe, "An Analytical and Experimental Investigation of Helicopter Rotor Hover Performance and Wake Geometry Characteristics," USAAMRDL Technical Report 71–24, June 1971.

6. F. X., Caradonna and C. Tung, "Experimental and Analytical Studies of a Model Helicopter Rotor in Hover, " NASA–TM–81232, 1981.

7. T. W. Roberts, "Computational of Potential Flows with Embedded Vortex Rings and Applications to Helicopter Rotor Wakes," NASA–CR–166542, 1983.

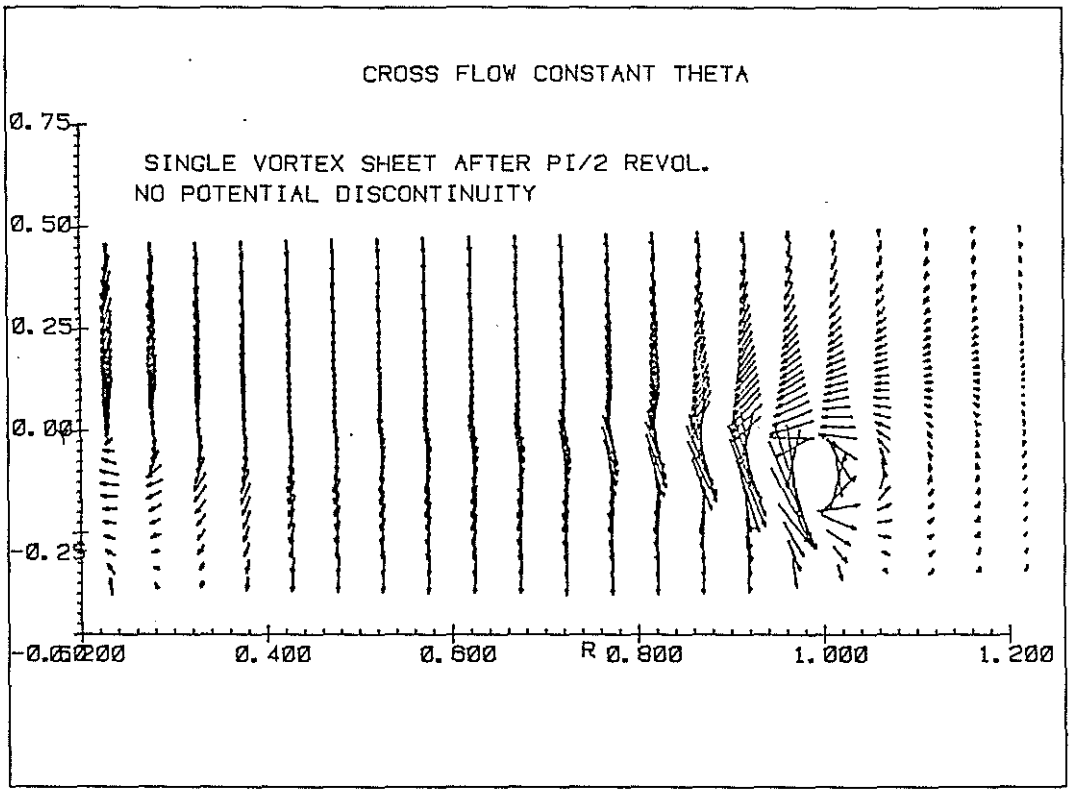

FIGURE -1

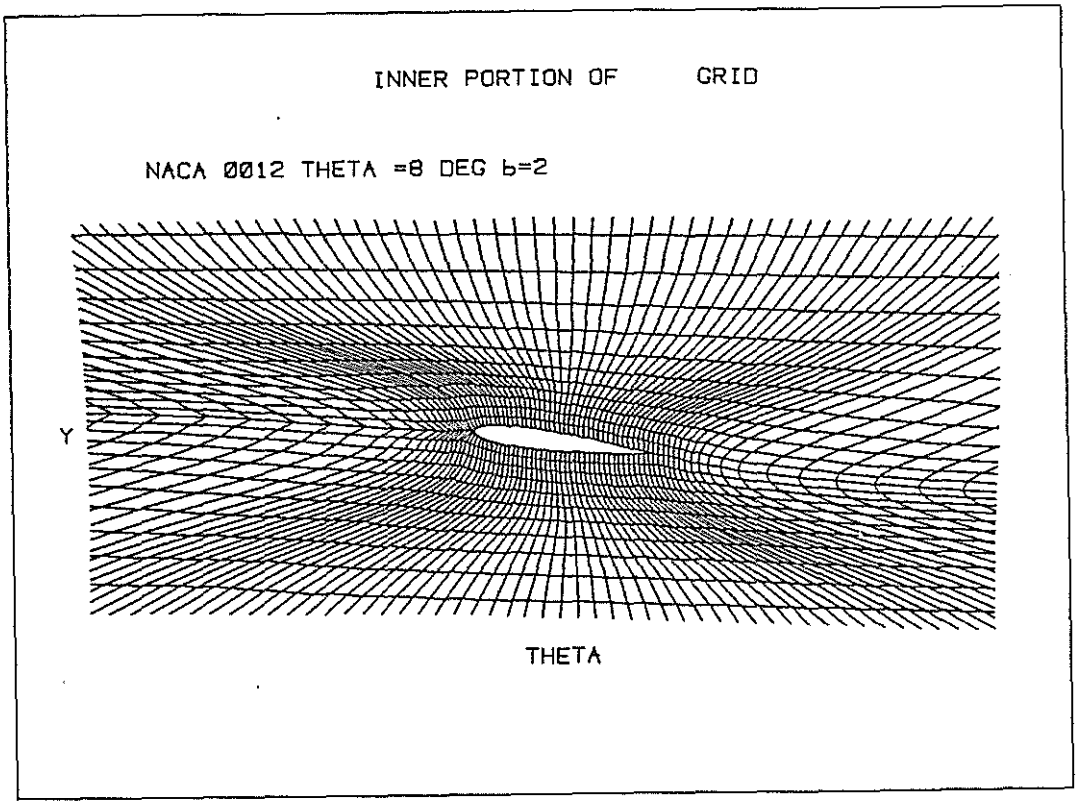

FIGURE -2

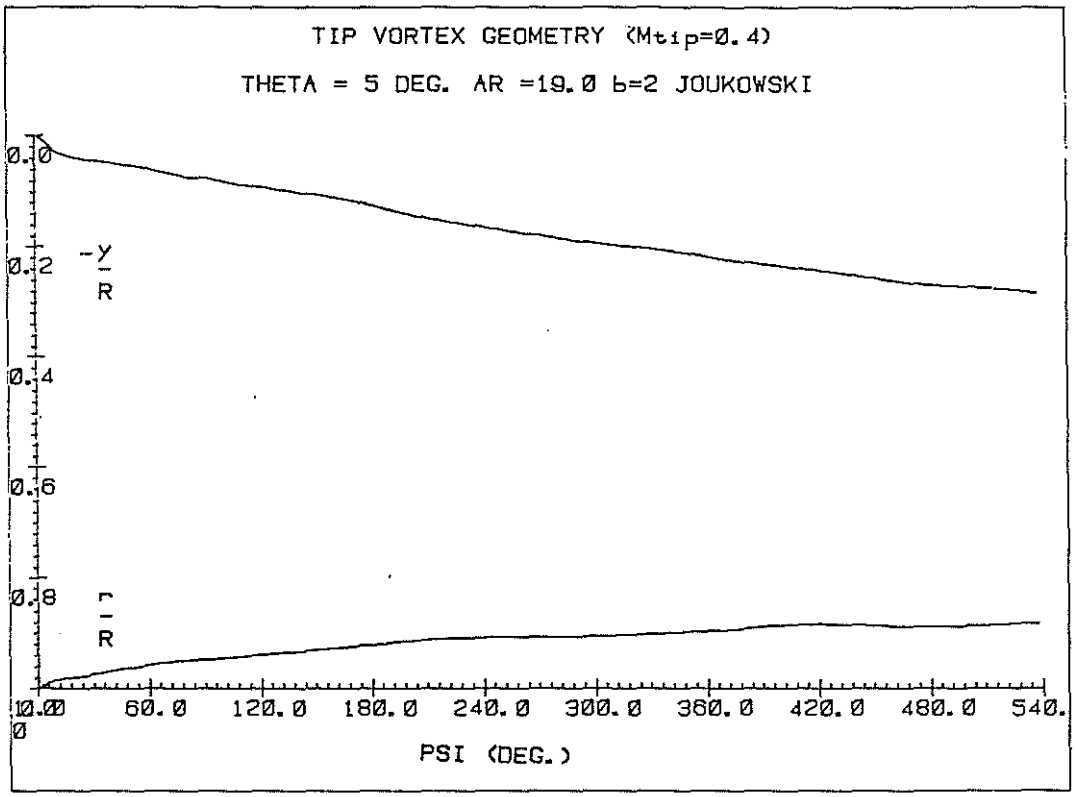

FIGURE -3

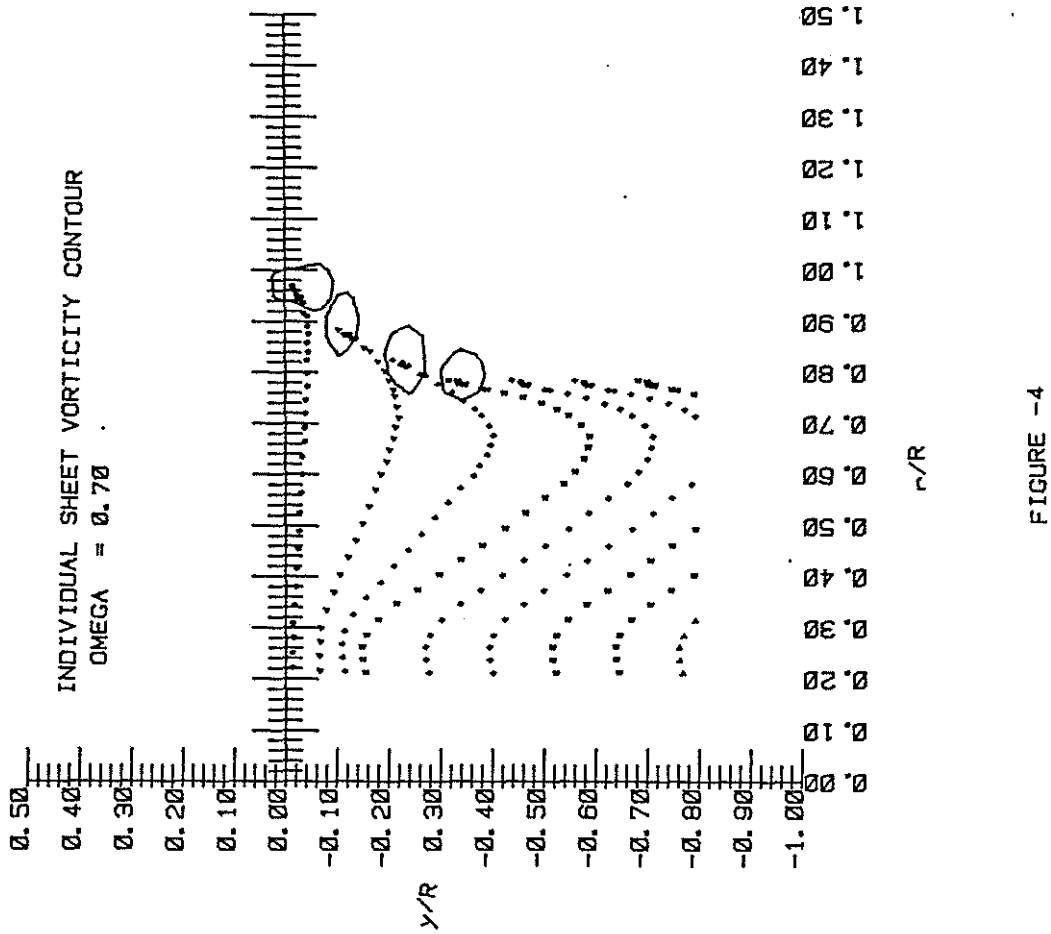

FIGURE -4

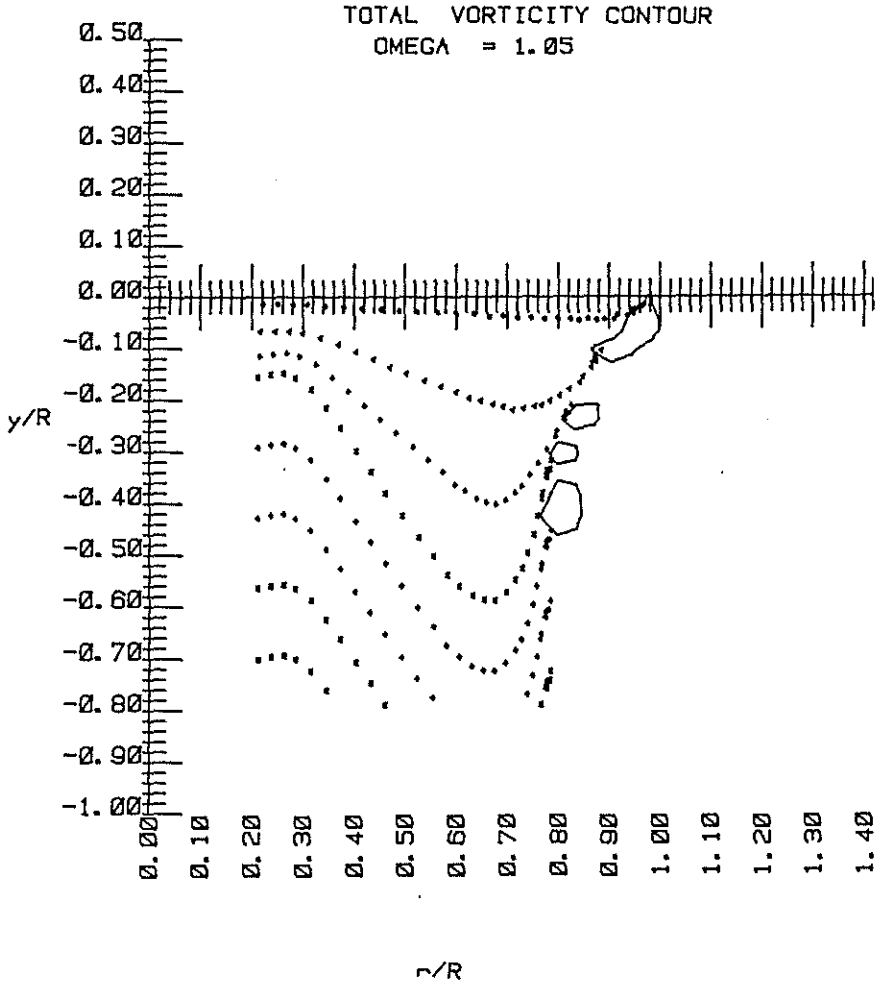

FIGURE -6

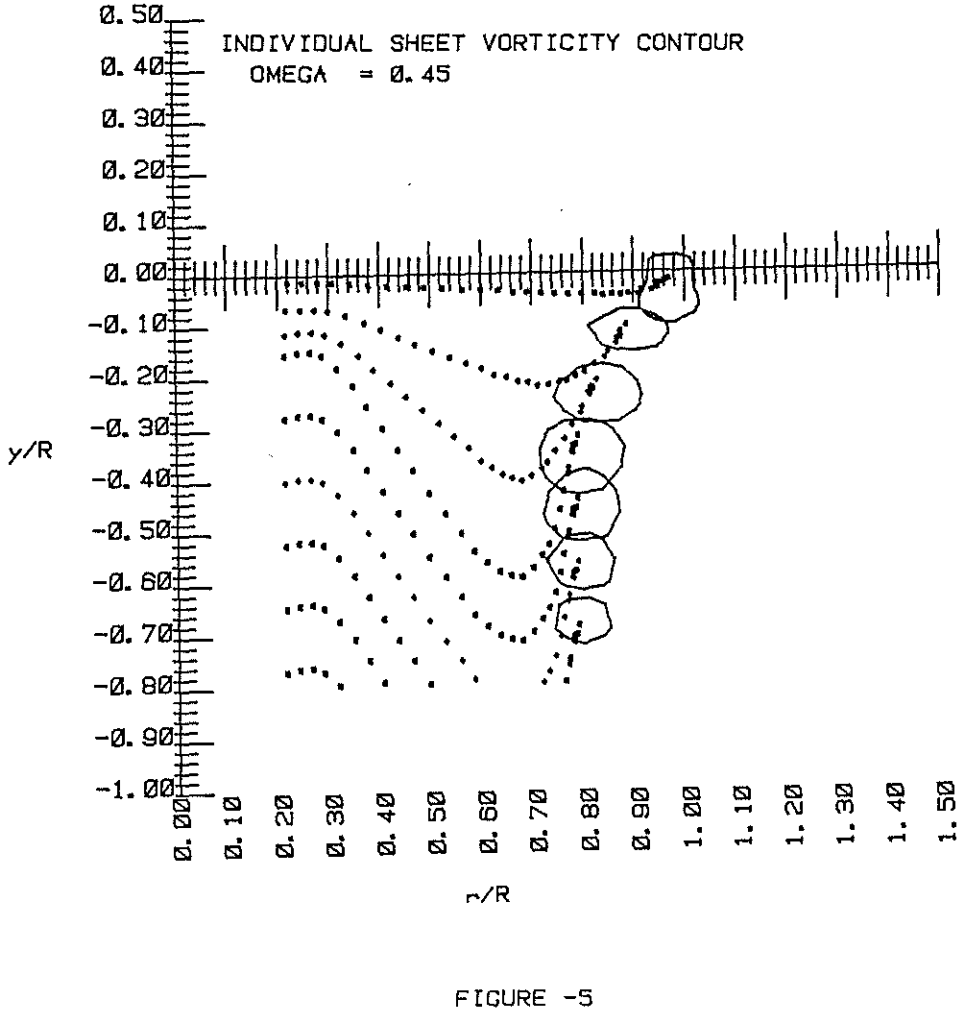

FIGURE -5

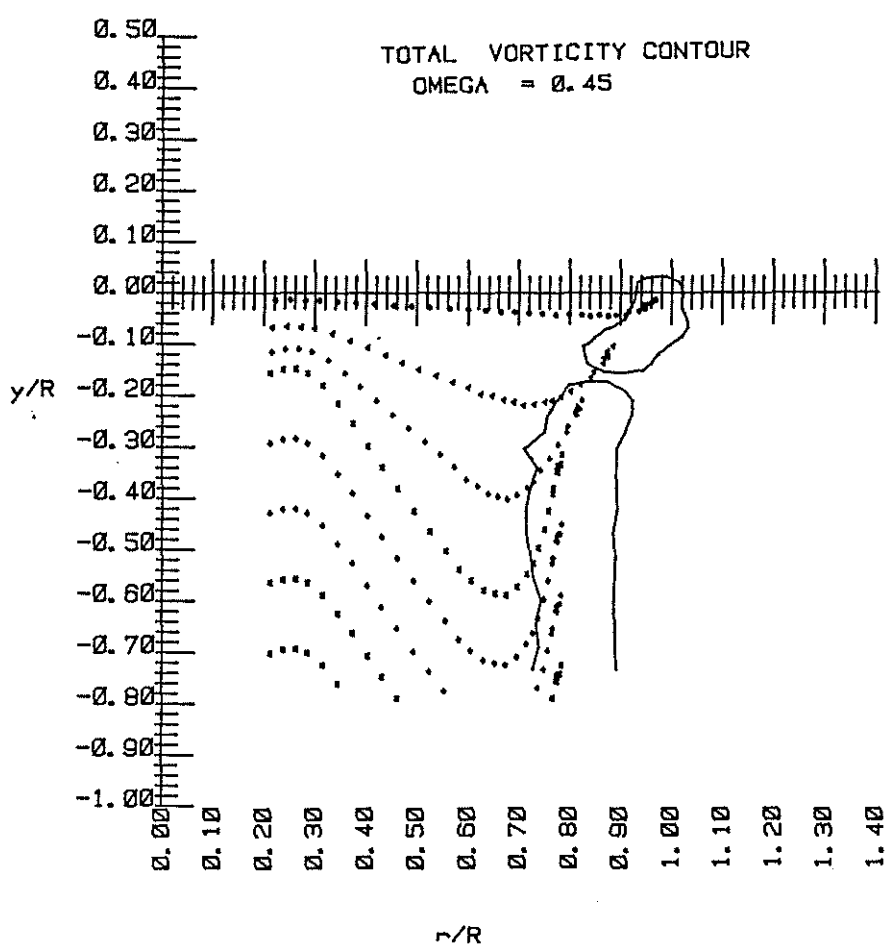

FIGURE -8

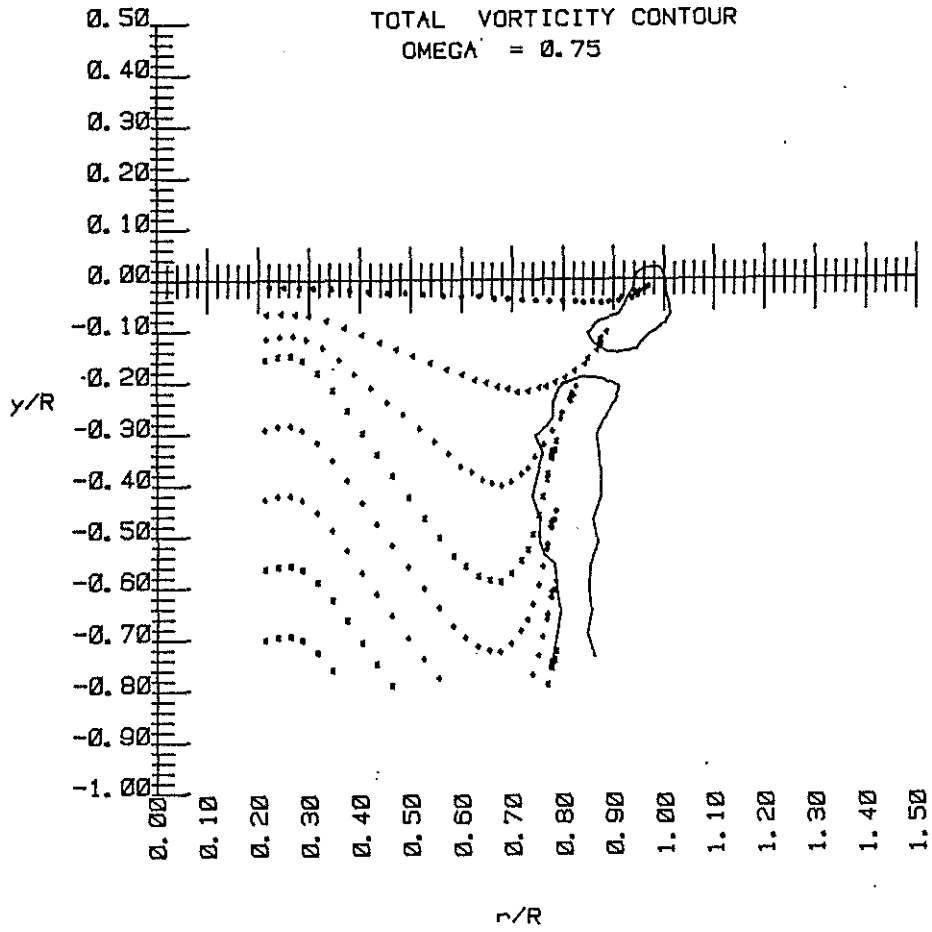

FIGURE -7

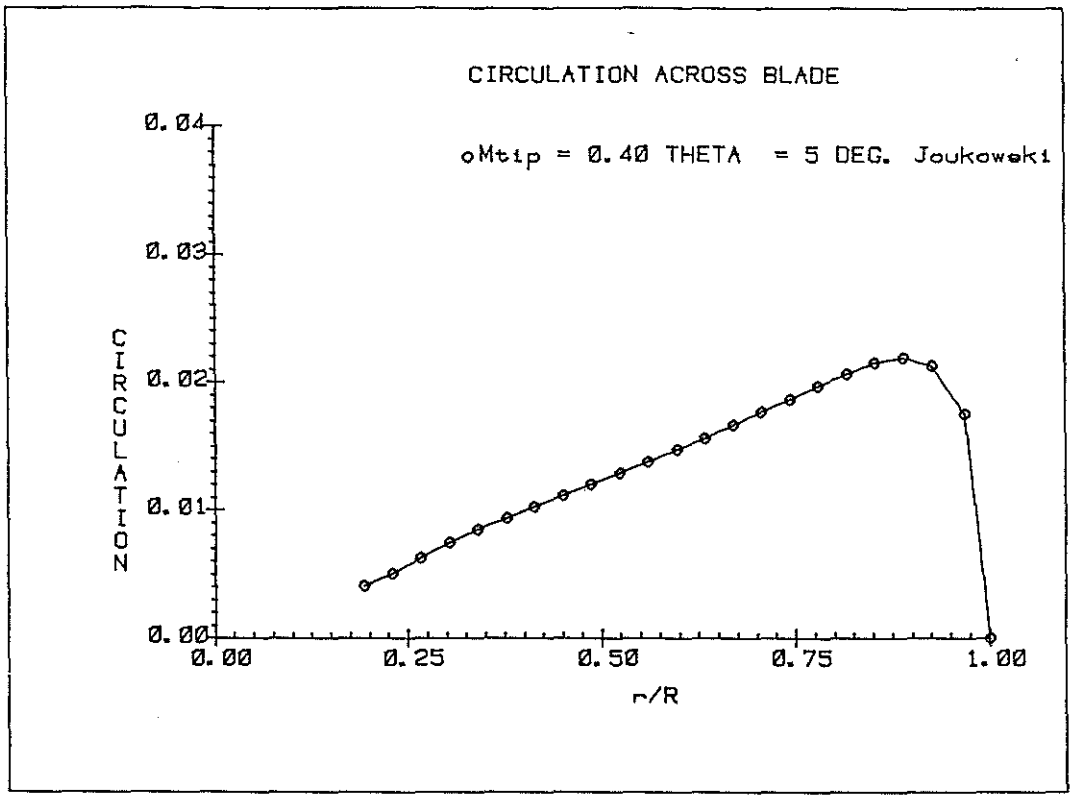

FIGURE -9

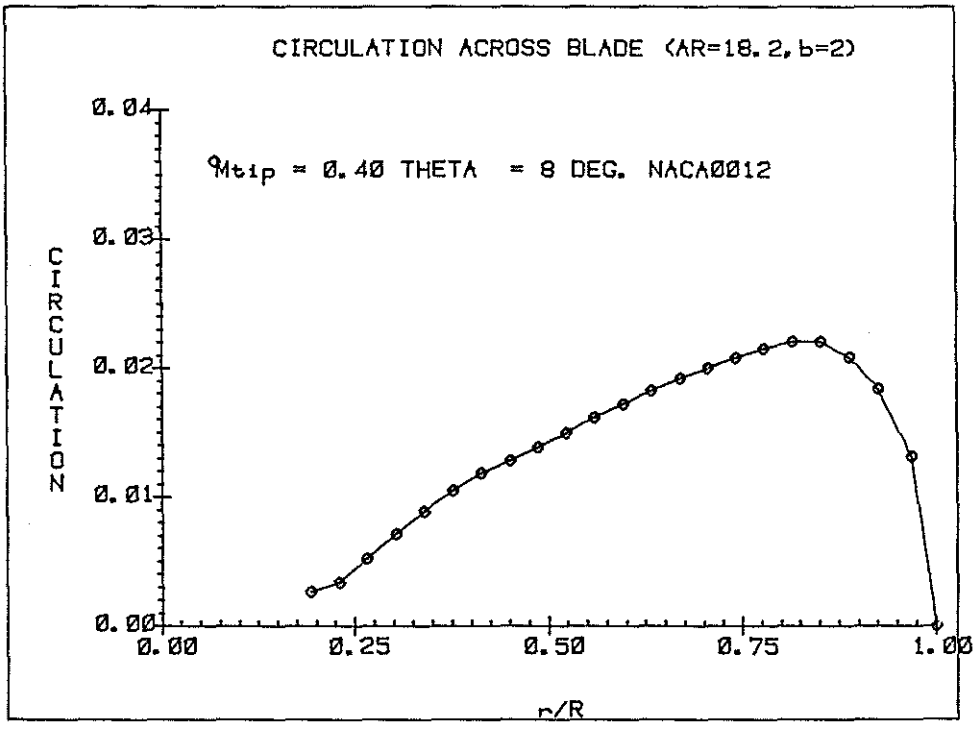

FIGURE -10

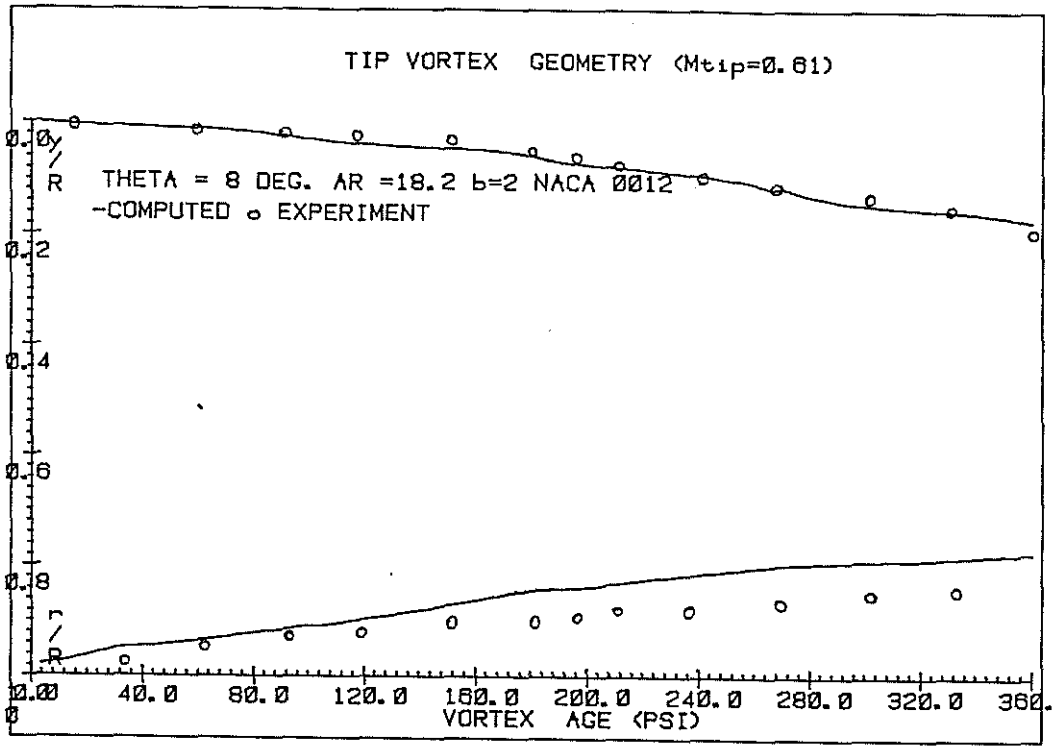

FIGURE -11

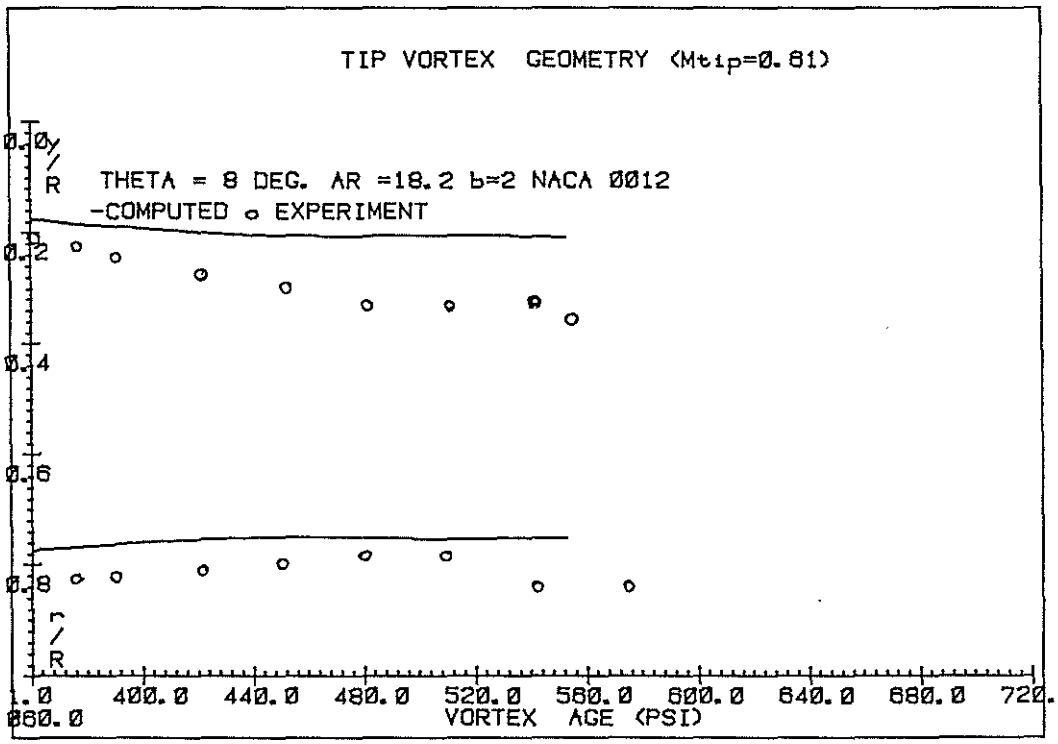

FIGURE -12

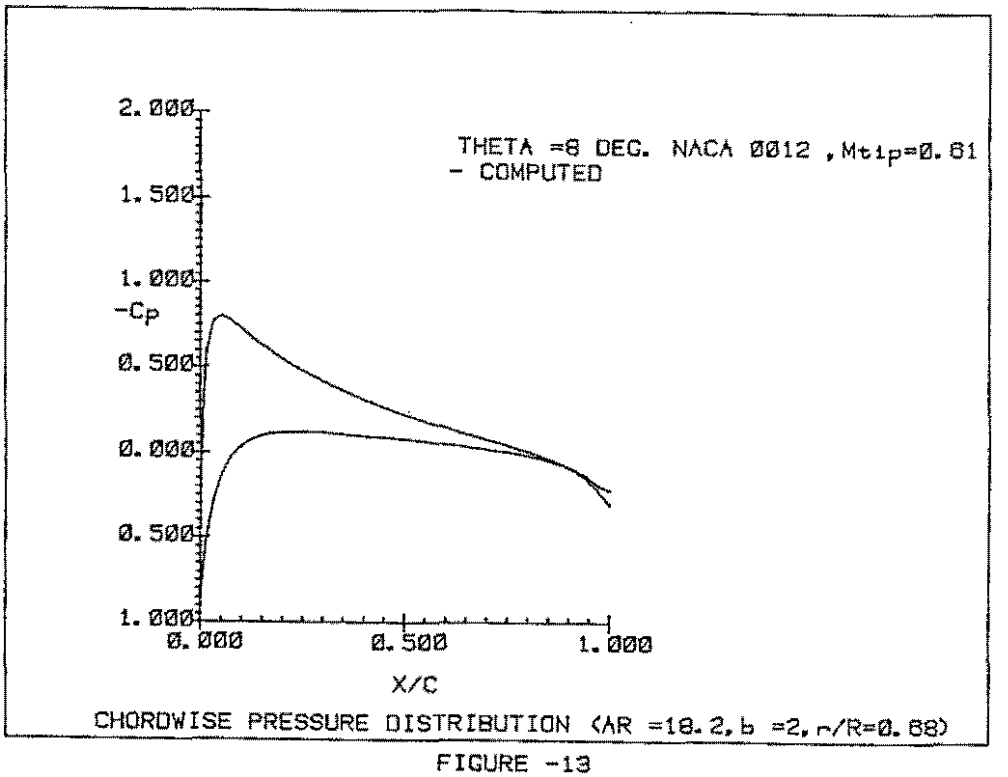

FIGURE -13

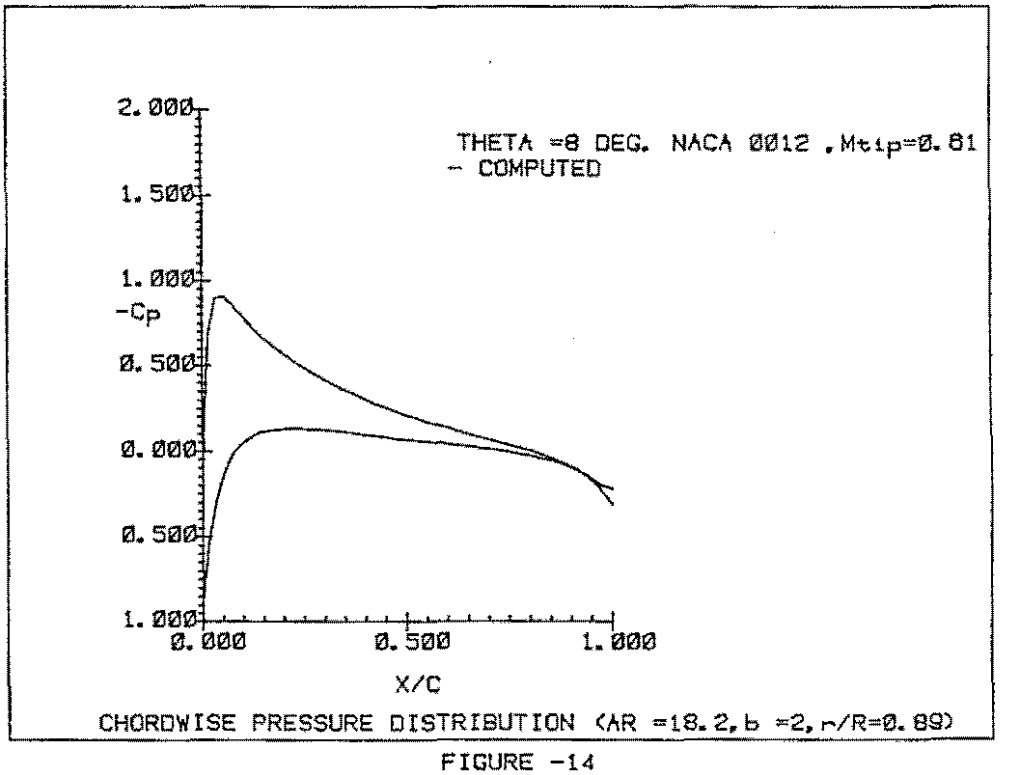

FIGURE -14

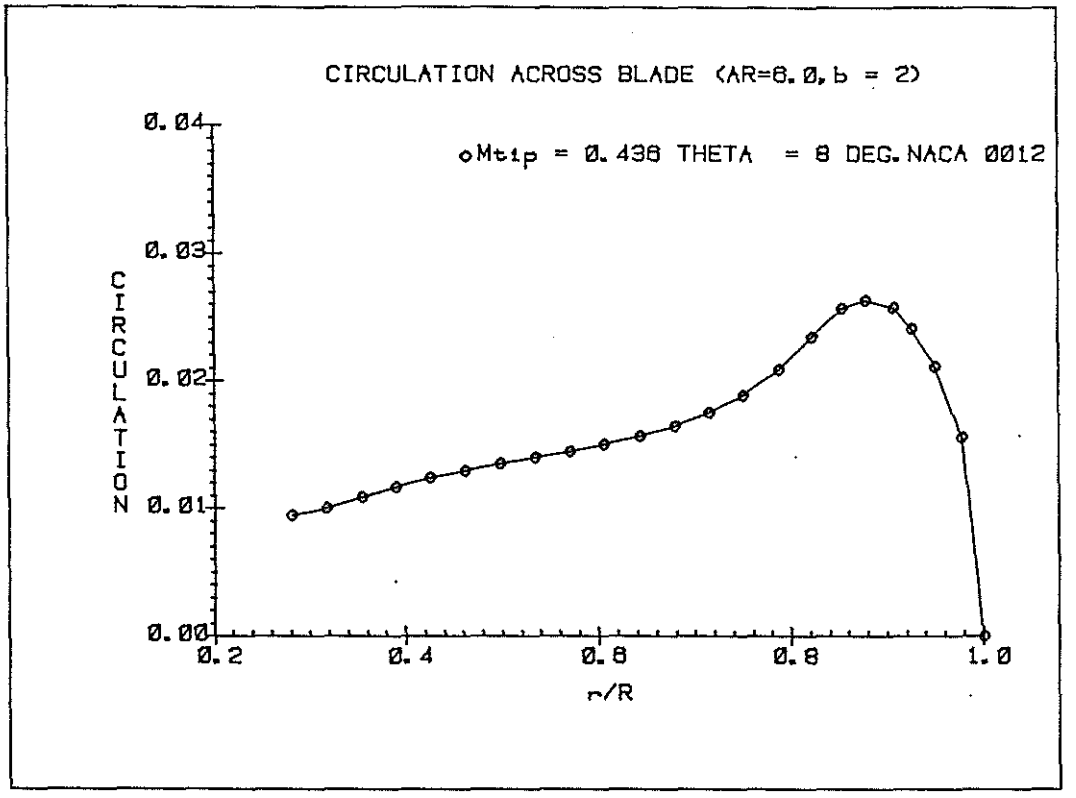

FIGURE -15

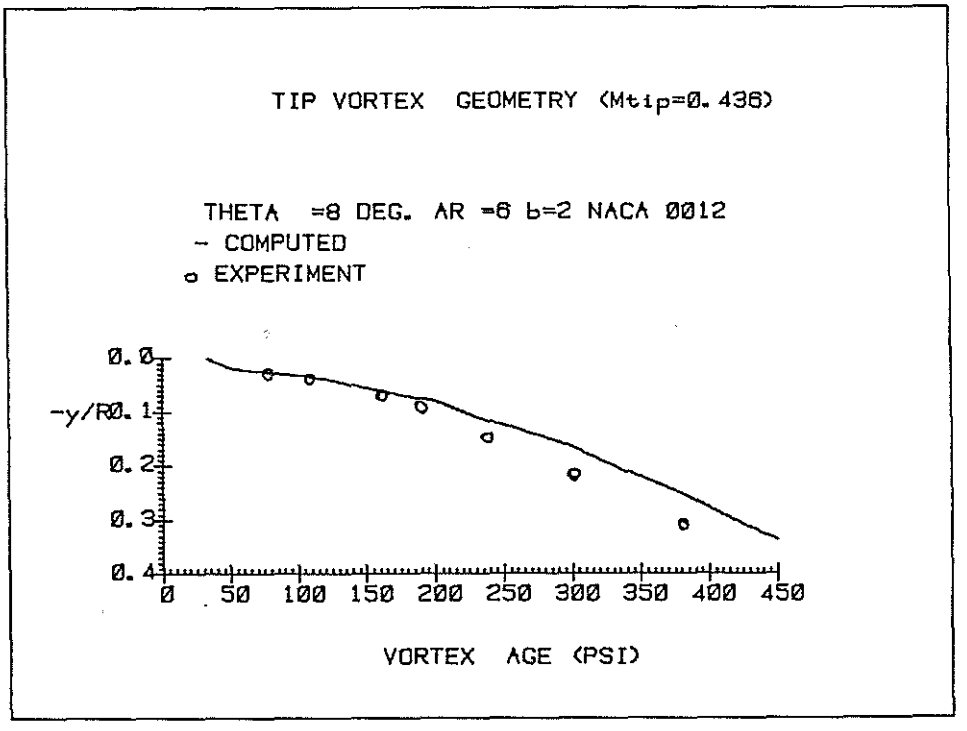

FIGURE -16

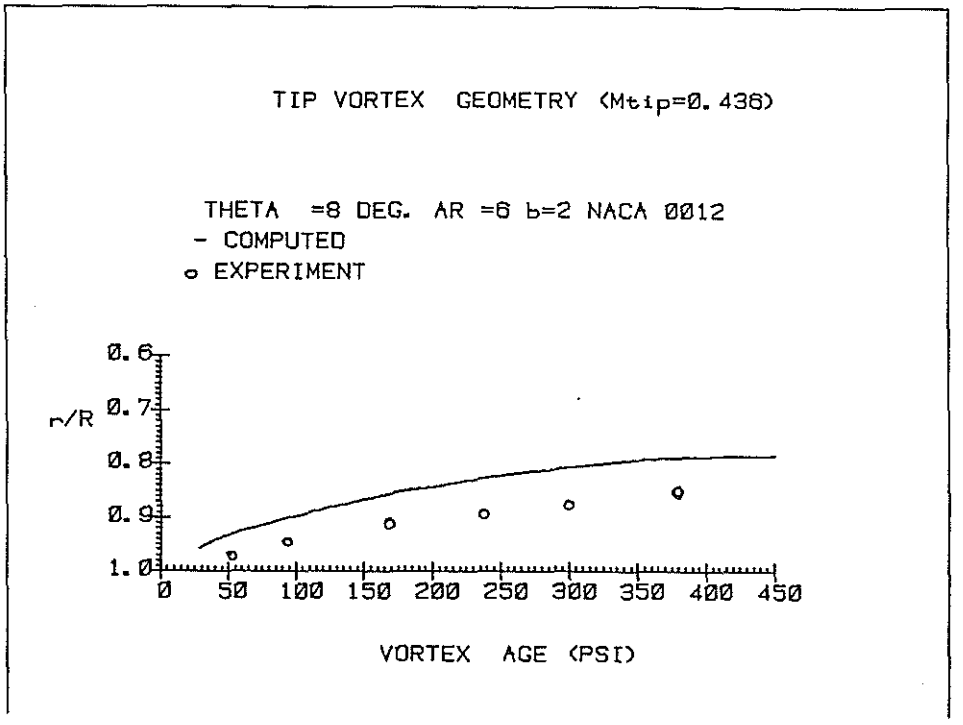

FIGURE -17

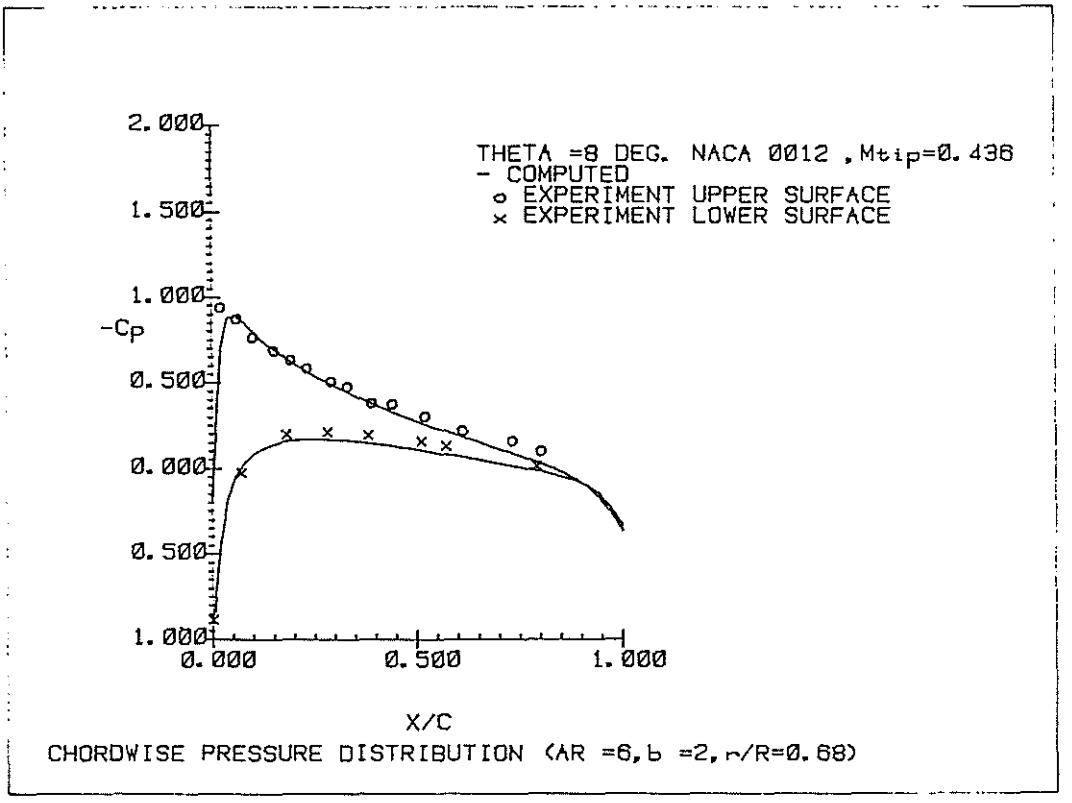

FIGURE -18

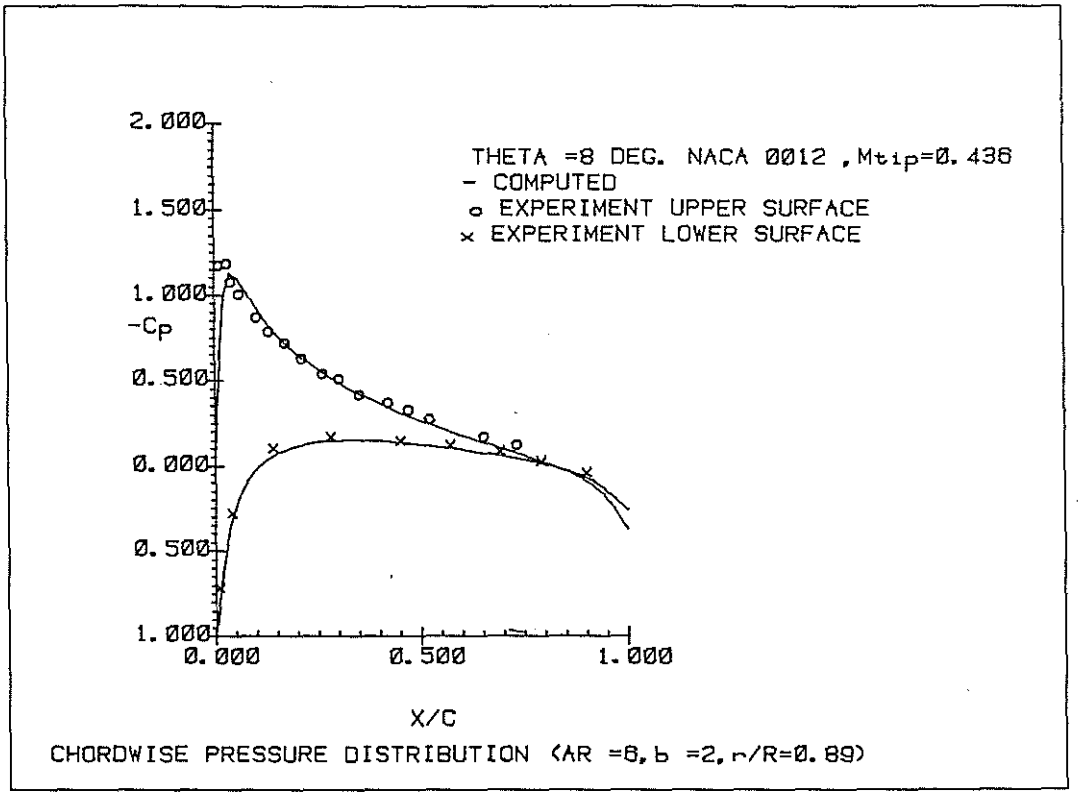

FIGURE -19

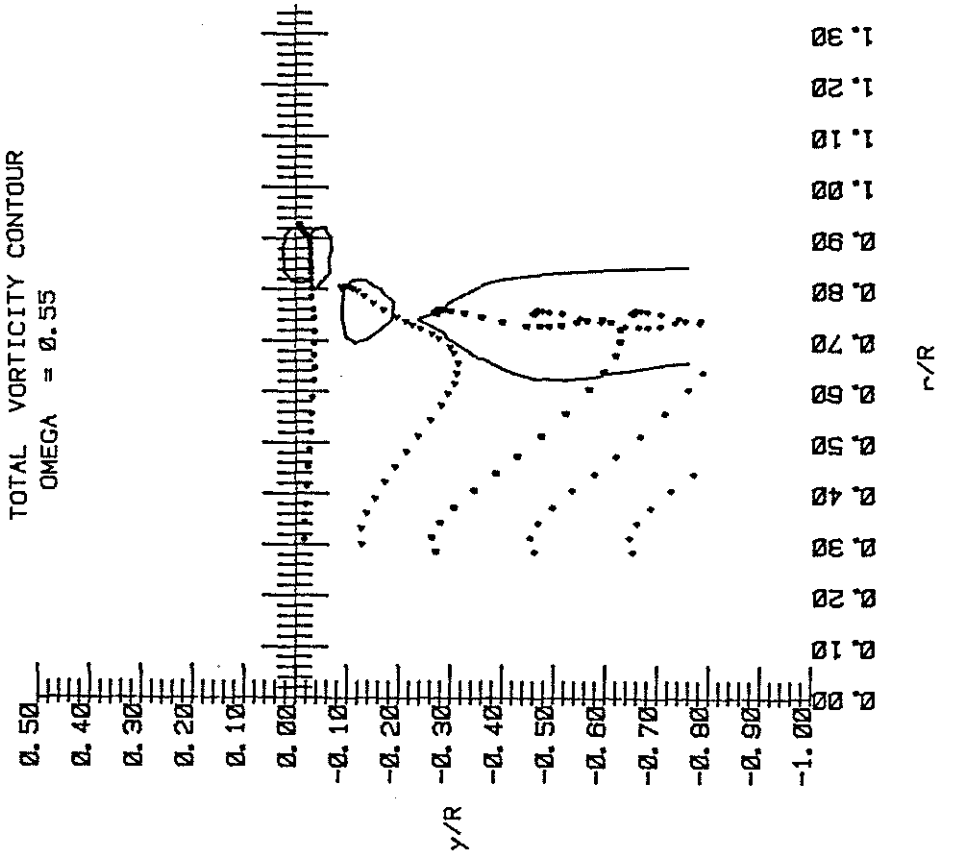

FIGURE -20

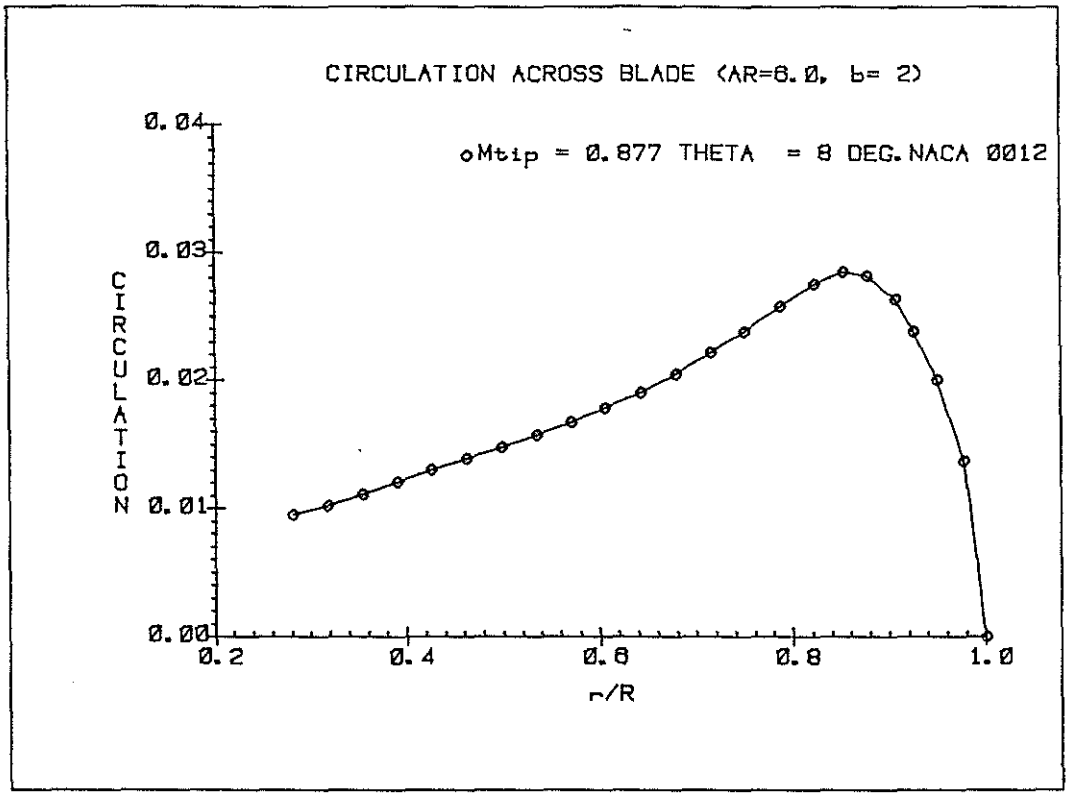

FIGURE -21

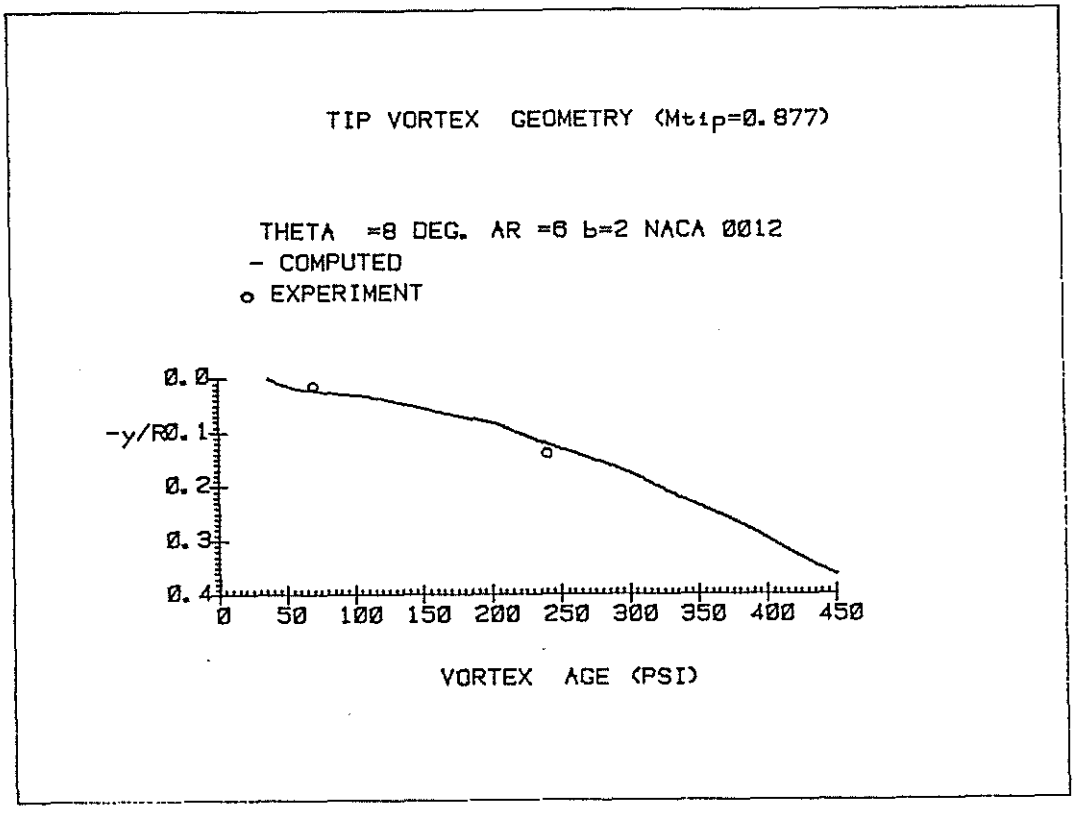

FIGURE -22

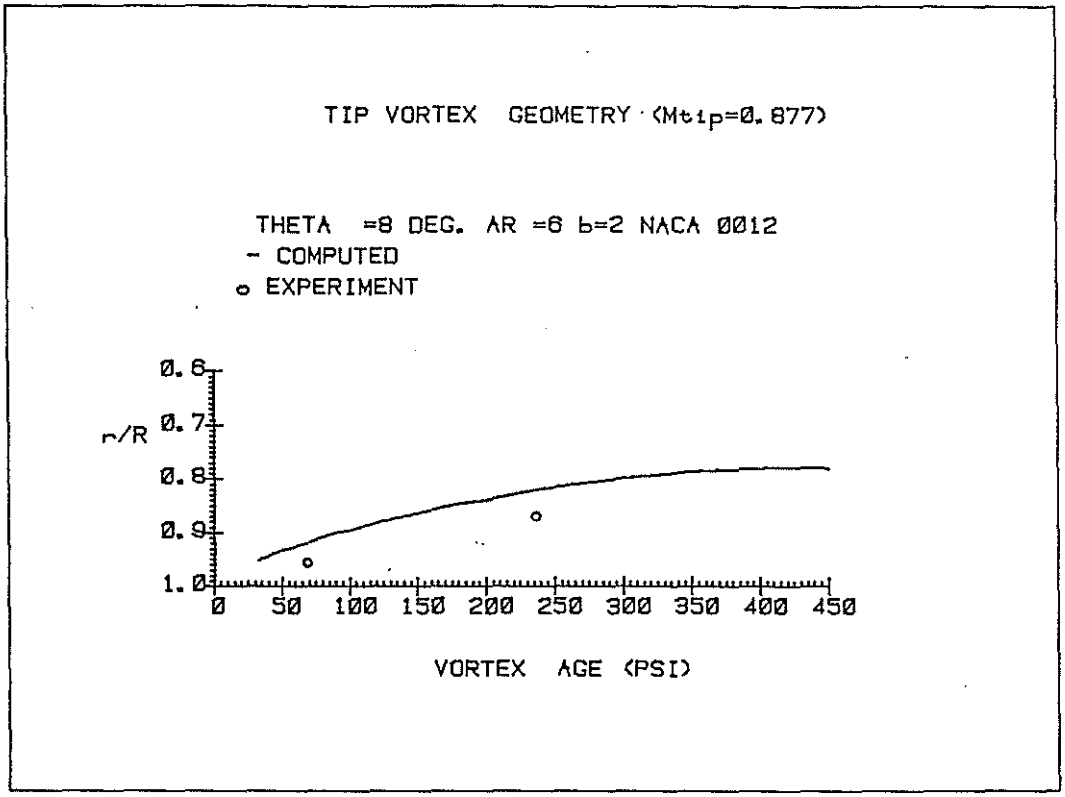

FIGURE -23

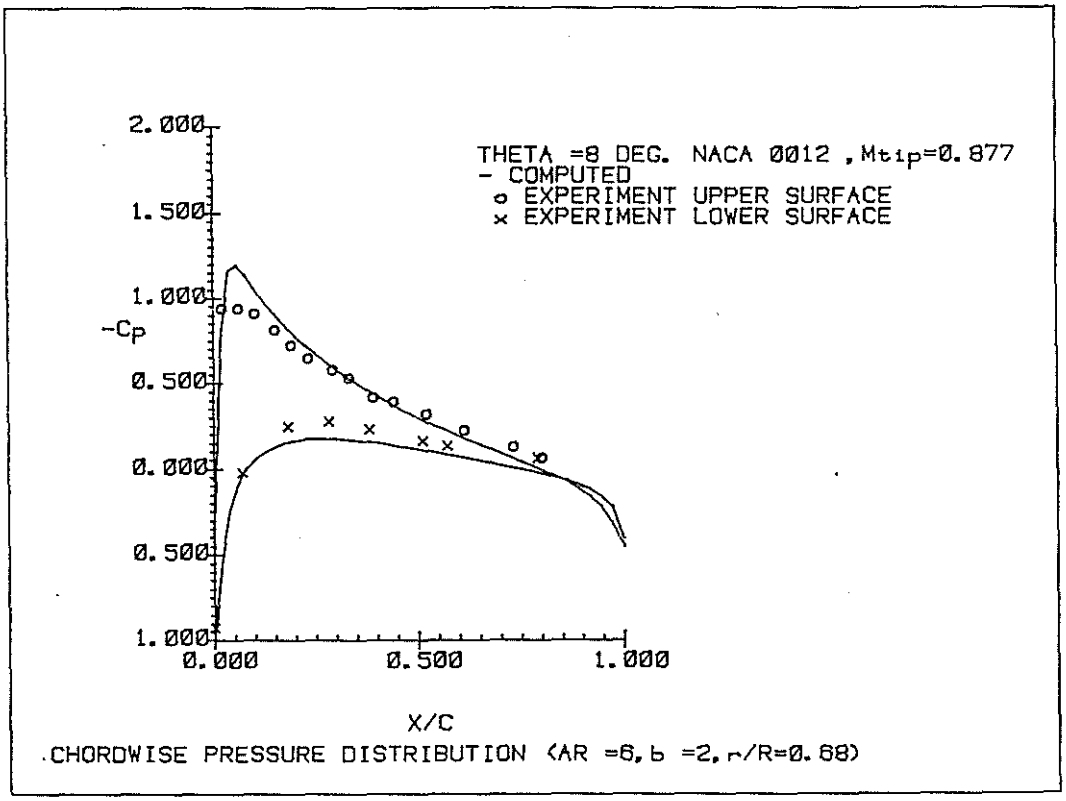

FIGURE -24

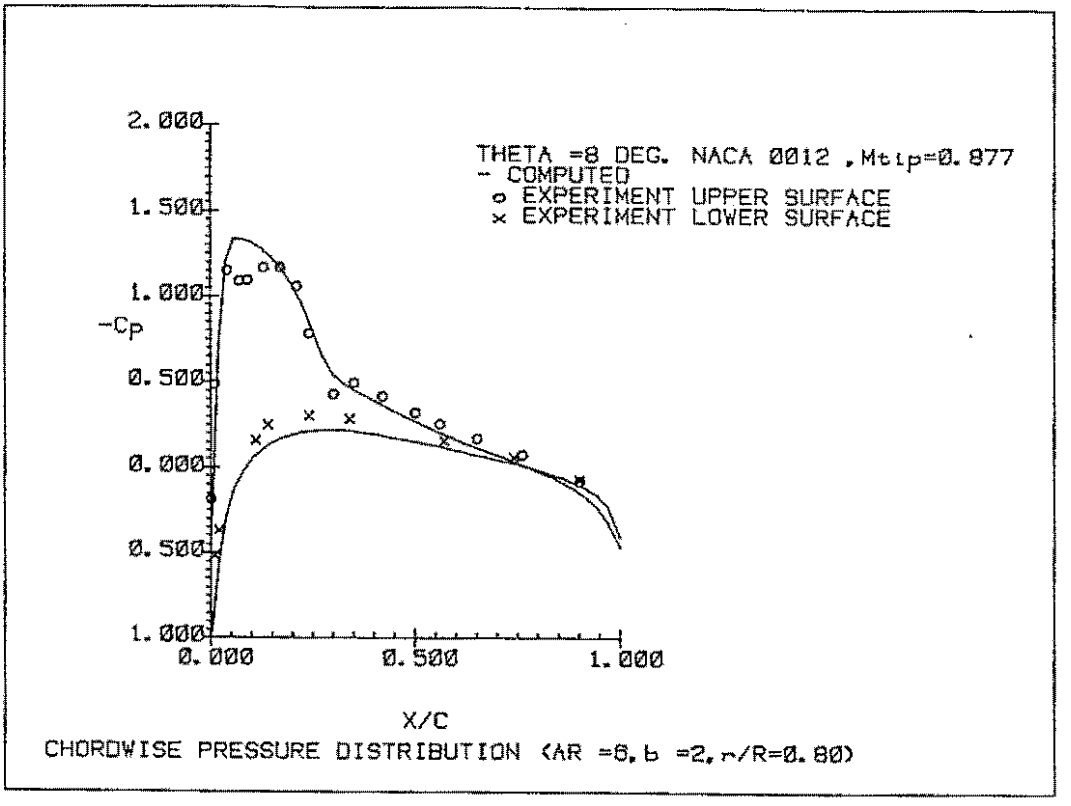

FIGURE -25

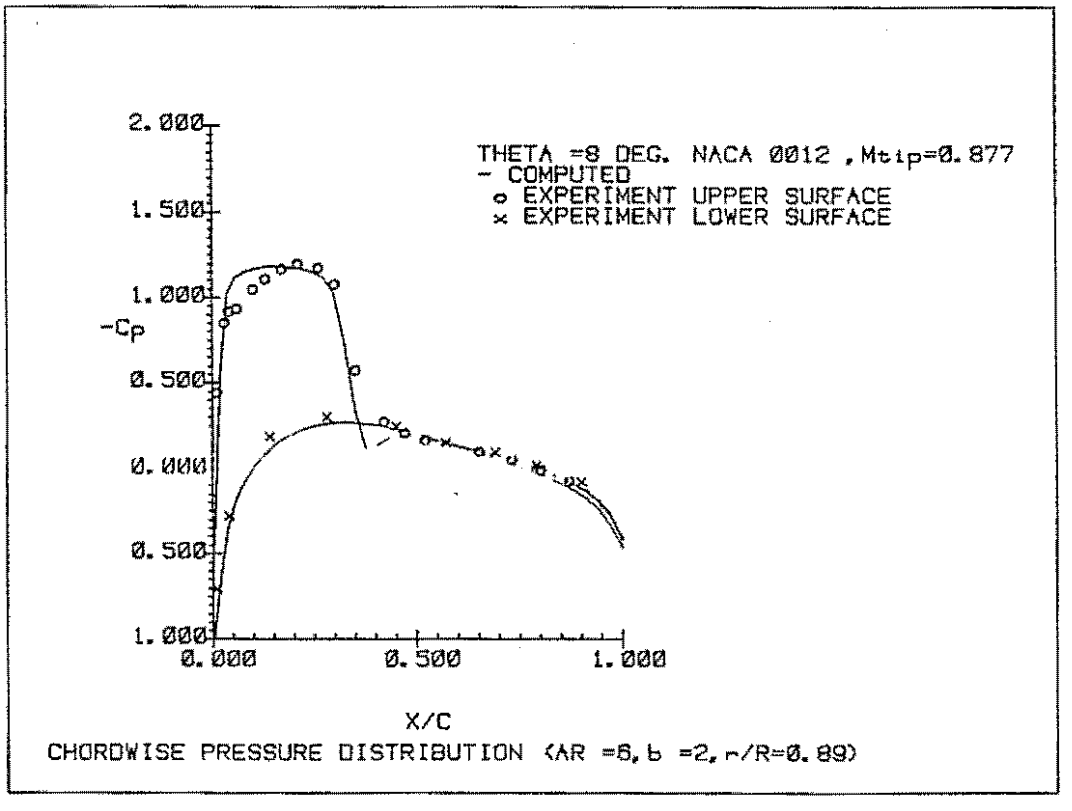

FIGURE -26

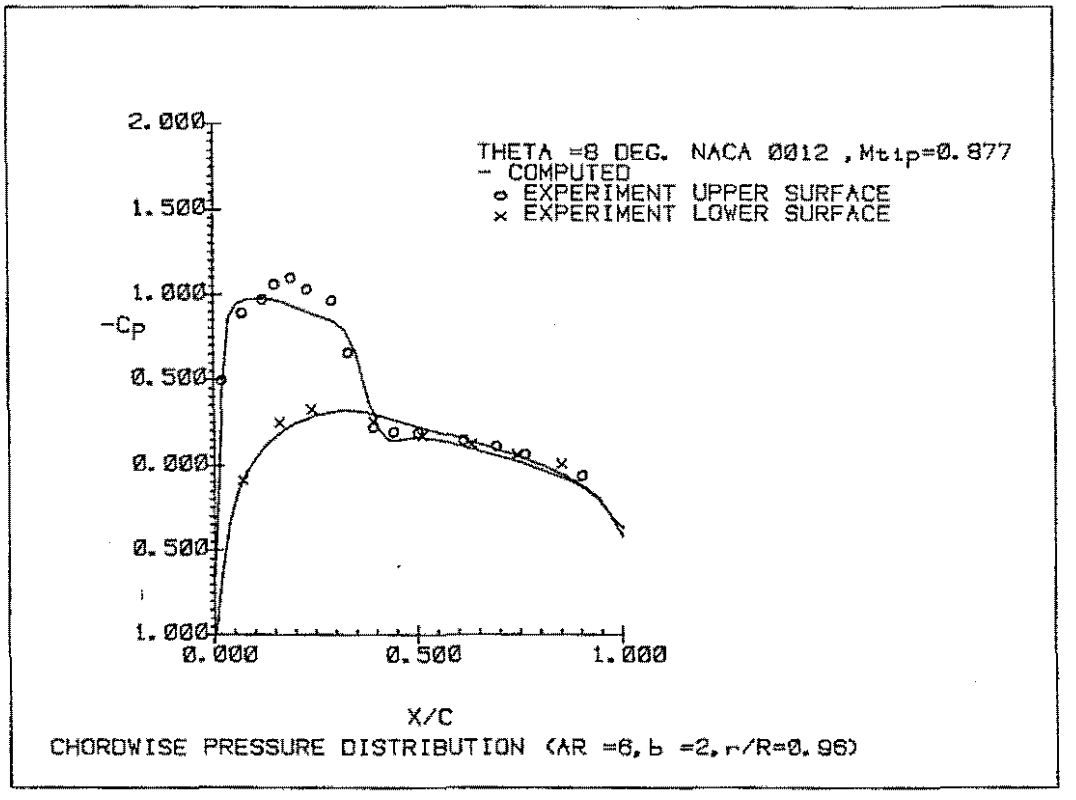
THETA =8 DEG. NACA 0012 , Mtip=0.877
- COMPUTED
o EXPERIMENT UPPER SURFACE
x EXPERIMENT LOWER SURFACE
2.000
1.500
1.000
-Cp
0.500
0.000
0.500
1.000
0.000
0.500
1.000
X/C
CHORDWISE PRESSURE DISTRIBUTION (AR =6, b =2, r/R=0.96)

FIGURE -27